Dissociation of H$_2$O at the vacancies of single-layer MoS$_2$

C. Ataca and S. Ciraci[*]

*UNAM–National Nanotechnology Research Center, Institute of Materials Science and Nanotechnology, and
Department of Physics, Bilkent University, Ankara 06800, Turkey*

Based on first-principles density functional theory and finite temperature molecular dynamics calculations, we predict that H$_2$O can be dissociated into its constituents O and H at specific vacancy defects of single-layer MoS$_2$ honeycomb structure, which subsequently are bound to fourfolded Mo and twofolded S atoms surrounding the vacancy, respectively. This exothermic and spontaneous process occurs, since the electronegativity and ionization energy of Mo are smaller than those of H. Once desorbed from twofolded S atoms, H atoms migrate readily on the MoS$_2$ surface and eventually form free H$_2$ molecules to be released from the surface. Present results are critical for acquiring clean and sustainable energy from hydrogen.

PACS number(s): 88.30.−k, 88.20.fn, 84.60.−h

I. INTRODUCTION

The utilization of hydrogen as a clean and sustainable energy source critically depends on the efficient production of H$_2$ molecules.[1] Since the reserves of free H$_2$ cannot occur in nature, hydrogen has been used as an energy carrier. Despite recent advances in developing high-capacity and safe hydrogen storage mediums[2–5] based on Dewar-Kubas[6] interactions, the production of H$_2$ is still a major goal of researchers in hydrogen economy. Presently, studies under the context of hydrogen evaluation reaction (HER)[7] aim to split H$_2$O to produce H$_2$ molecules. In plants, the analog of HER is catalyzed by nitrogenase and hydrogenase enzymes. These enzymes include Mo and S atoms at their active sites. Many researchers conducted experiments and theoretical calculations on HER properties of MoS$_2$.[8–15] Before the HER process, protons are obtained from electrochemical splitting of water. To this end usually two catalysts, such as Ru/SrTiO$_3$ or (Ga$_{1-x}$Zn$_x$)(N$_{1-x}$O$_x$) powder are used as a photocatalyst to split H$_2$O by treating O and H separately.[16–19] After these reactions, a HER takes place and supplies electrons to protons to form a H$_2$ molecule. Under these circumstances, the undesired reformation of H$_2$O cannot be avoided.

Owing to its important role in HER, active edges of MoS$_2$ nanoparticles have been the subject of many studies.[20–22] After the first synthesis of a single-layer MoS$_2$ honeycomb structure[23] (which is specified as 1H-MoS$_2$), the unusual chemical and electronic properties of its flakes and nanoribbons have been revealed.[24–27] In particular, 1H-MoS$_2$ is mechanically a stiff material.[26] In contrast to graphene, it is a semiconductor suitable for nanotransistor fabrication.[28] They can form a multilayer structure due to weak van der Waals attraction. Direct-indirect band-gap transition with the number of layers leads to interesting photoluminescence properties.[23,29] Because of the high stiffness of MoS$_2$, the stick-slip process in the sliding of 1H-MoS$_2$-coated surfaces is suppressed and ultralow friction is attained.[30] Different types of defects, such as Mo- and S-vacancy, MoS- and S$_2$-divacancy, MoS$_2$-triple vacancy, and reconstructed armchair and zigzag edges can occur in 1H-MoS$_2$.[24,25] While the equilibrium concentrations of these vacancies are found to be very low owing to their high formation energies, new techniques have been developed to generate vacancy defects in the nonequilibrium state, as well as the nanomeshes of vacancies and holes.[31–33]

In the present study we reveal an important feature involved in the interaction between H$_2$O and 1H-MoS$_2$. We show that a water molecule can be dissociated into its constituents O and 2H atoms at a MoS$_2$ vacancy in a single-layer MoS$_2$, which, in turn, are bound to Mo and S atoms around the vacancy, respectively. This process by itself is exothermic and spontaneous. Two crucial ingredients underlying this catalytic reaction are (i) The electronegativity of Mo is slightly smaller than that of H. According to Pauling scale the electronegativity of Mo and H is 2.16 and 2.20, respectively. (ii) The ionization energy of Mo is almost half of H (684 and 1312 KJ/mole, respectively). Once desorbed from S atoms, H atoms migrate on the MoS$_2$ surface and eventually form free H$_2$ molecules, which in turn, are released from the surface.

II. METHOD

Our predictions are based on first-principles density functional theory (DFT) using projector augmented wave potentials.[34] The exchange-correlation potential has been represented by the generalized gradient approximation characterized by Perdew-Burke-Ernzerhof[35] including van der Waals correction (vdW)[36] both for spin-polarized and spin-unpolarized cases. We used periodic boundary conditions, where local processes are treated with (4 × 4) supercells of 1H-MoS$_2$. Supercell size, kinetic energy cutoff, and Brillouin zone (BZ) sampling of the calculations have been determined after extensive convergence analysis. A large spacing of ∼15 Å between two-dimensional (2D) single layers is taken to prevent interlayer interactions. A plane-wave basis set with a kinetic energy cutoff of 520 eV is used. In the self-consistent field potential and total energy calculations BZ is sampled by special **k**-points. The numbers of these **k**-points are (37 × 37 × 1) for the primitive MoS$_2$ unit cell and are scaled according to the size of the supercells. All atomic positions and lattice constants are optimized by using the conjugate gradient method, where the total energy and atomic forces are minimized. The convergence for energy is chosen as 10^{-6} eV between two consecutive steps, and the maximum Hellmann-Feynman forces acting on each atom is less than 0.01 eV/Å upon ionic relaxation. The pressure in the unit cell

is kept below 5 kbar. Bader analysis[37] is used to calculate the charge on atoms. Numerical calculations have been performed by using VASP software.[38] Frequencies of phonon modes are calculated using small displacement method (SDM)[39] in terms of forces calculated from first principles.

III. INTERACTION OF H₂O MOLECULE WITH 1H-MoS₂

In this section we present the analysis of physical and chemical processes leading to the dissociation of a H_2O molecule at MoS_2 vacancy and other phenomena taking place thereafter. These are the binding of OH to a Mo atom and H to a S atom surrounding the vacancy at the initial stage of dissociation and later the binding of the second H split from OH to another S atom leaving behind an O atom, which remained attached to the same Mo atoms. Furthermore, we also examine the diffusion of H atoms on the surface of MoS_2 subsequent to its dissociation from S-H bonds.

We start with a brief description of the 1H-MoS₂ single-layer honeycomb structure, since the structure of 1H-MoS₂ was already treated earlier in Refs. 24–27 extensively.

1H-MoS₂ is a nonmagnetic semiconductor with a band gap of 1.63 eV (the experimental gap[23] is 1.90 eV; the band gap calculated using LDA[25] is 1.9 eV). In the top view, Mo and S₂ atoms alternatingly occupy the corners of the hexagons. It has a 2D hexagonal lattice structure, which has Mo and S₂ atoms in the primitive unit cell. The lattice parameters are calculated to be $a = b = 3.19$ Å, $d_{S-S} = 3.12$ Å (which corresponds to the thickness of the MoS₂ layer), $d_{Mo-S} = 2.42$ Å, and $\alpha_{S-Mo-S} = 80.52°$. Each Mo atom is sixfolded forming directional bonds with six nearest-neighbor S atoms; each S atom is threefolded forming directional bonds with three nearest-neighbor Mo atoms. Accordingly, single-layer 1H-MoS₂ consists of three atomic planes: the Mo atomic plane is between the top and bottom S atomic planes. Structural parameters predicted and used in this study are in agreement with available experimental data. The calculation of structural, electronic, magnetic, and mechanical properties of 1H-MoS₂ and the comparison of calculated values with available experimental data have been performed by Ataca *et al.*[24–27] In these studies the differences between 2D 1H-MoS₂ and three-dimensional (3D) layered crystal 2H-MoS₂ and various dimensionality effects have been
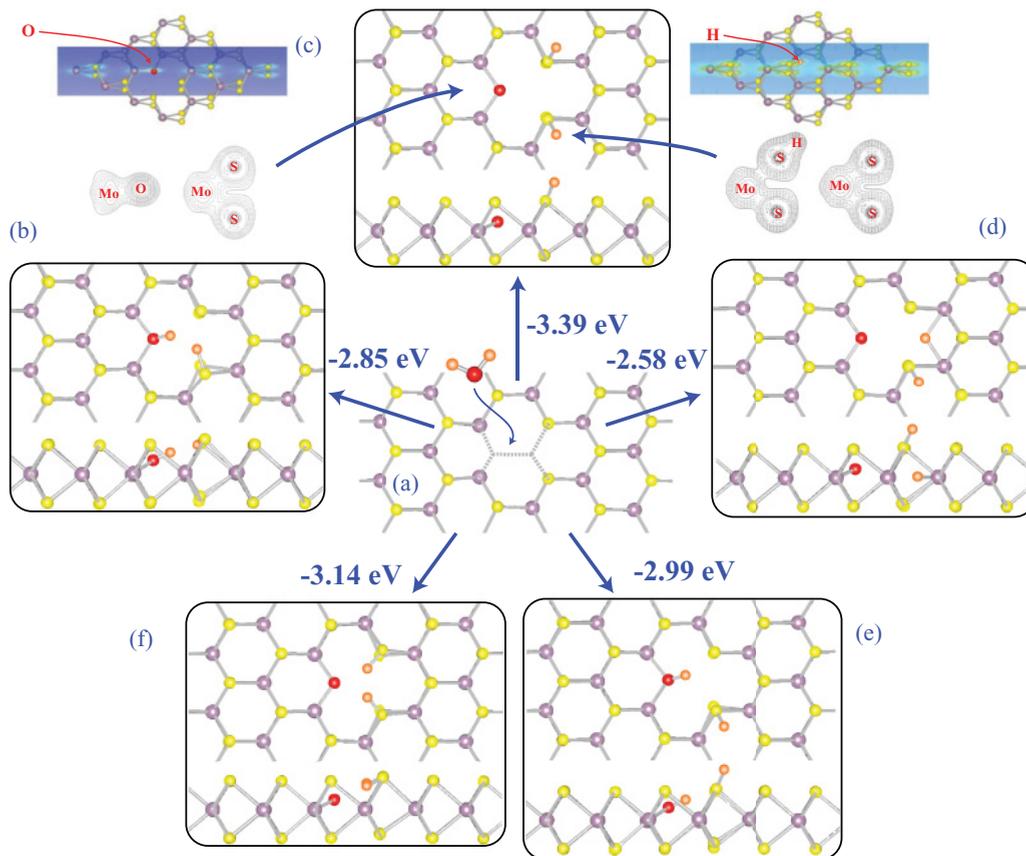

FIG. 1. (Color online) Dissociation of water molecule trapped in a MoS₂ triple vacancy of 1H-MoS₂. (a) A free H₂O is approaching the MoS₂ triple vacancy. Purple (large gray), yellow (light), red (dark), and orange (small light gray) balls indicate Mo, S, O, and H atoms, respectively. (b) The precursor state occurs upon structure optimization and leads to the spontaneous dissociation of H₂O into OH and H in an exothermic process. This state has the total energy, which is −2.85 eV lower relative to (a). (c) The most energetic (lowest energy) state, which occurred through *ab initio* MD calculations at $T = 1000$ K initiating from (b), where a H atom is split from OH and is adsorbed to a twofolded S atom surrounding the vacancy leaving behind an O atom adsorbed to two fourfolded Mo atoms. This state has −3.39 eV energy relative to (a). The contour plots of total charge density of various bonds on various planes are presented on the right- and left-hand sides. (d), (e), and (f) are other intermediate states, which occur in the course of *ab initio* MD calculation. Each panel presents both top and side views of atomic configurations.

treated. Structural parameters optimized in the present paper are in good agreement with those reported earlier, as well as with those values which are reported experimentally.[24–27]

According to Bader analysis,[37] the effective charges of Mo and S atoms are $+1.0e$ and $-0.5e$, respectively. In this respect, 1H-MoS₂ can be viewed as a positively charged Mo atomic plane sandwiched between two negatively charged S planes. The same analysis results in effective charges of $-1.30e$ and $+0.65e$ on O and H atoms of the water molecule, respectively. As a result, a repulsive interaction sets in between free H₂O and the perfect surface of 1H-MoS₂. No matter what its initial orientation is, H₂O first rotates so as two H atoms face the negatively charged S plane and subsequently it is repelled. However, an attractive interaction and hence a chemical bonding with H₂O can be attained only when a hole is opened at the S plane through vacancy defects. In the case of S and S₂ (i.e., single S atom vacancy at each surface) vacancies, the size of the vacancy does not allow H₂O to interact with positively charged Mo atoms. Even if the vacancy of two adjacent S atoms in the same S plane allows H₂O to engage in an attractive interaction, the configuration of the water molecule remains intact owing to its weak binding of 0.59 eV. Similarly, MoS divacancy also attracts H₂O and even splits it into OH and H, which are bound to Mo and S atoms surrounding the vacancy. However, dissociating H from OH does not take place, since the O atom cannot receive sufficient electrons in order to release H. Also, the edges of 1H-MoS₂ were not found active enough to split H₂O.

A. Dissociation of H₂O at MoS₂ vacancy

Remarkably, the surrounding of MoS₂ triple vacancy is found to be a suitable medium for the dissociation of H₂O, where a strong chemical interaction with H₂O is achieved to exchange electrons with neighboring Mo atoms leading to the separation of H and O atoms. In fact, a MoS₂ vacancy attracts

a free H₂O molecule, even if it is already ∼3 Å away from the S plane. Initially, a H₂O molecule is trapped in the vacancy by forming bonds with two fourfold Mo atoms each having two unsaturated dangling bonds due to missing S₂. Once bound, the O atom of H₂O receives electrons from two Mo atoms and subsequently one H atom is released to be attached to one of the S atoms at close proximity leaving behind OH bound to two Mo atoms as described in Fig. 1(b). At the end, the total energy is lowered by 2.85 eV [relative to the energy of free H₂O and 1H-MoS₂ with a MoS₂ vacancy, i.e. relative to Fig. 1(a)] and the effective charge on Mo increases to $+1.15e$. This exothermic process occurs spontaneously without an energy barrier and is a precursor to other states presented in Fig. 1, which lower the total energy further. Here, while the ionic Mo-O-Mo bonds are formed from the combination of d_{xz}, d_{yz}, and $d_{x^2+y^2}$ orbitals of Mo and p_x and p_y orbitals of O, the O-H bond, however, is dominated by p_z and p_x orbitals of O and the s orbital of the H atom.

We also carried out *ab initio* molecular dynamics (MD) calculations at $T = 1000$ K by normalizing the velocities after every 40 time steps, with each time step being 2.5 femtoseconds. The simulation temperature is taken high to speed up the statistics. Further to the atomic configuration in Fig. 1(b) attained through the structure optimization based on conjugate gradient, four different binding configurations described in Figs. 1(c)–1(f) are revealed at different intermediate stages of MD calculations. These configurations correspond to different minima in the Born-Oppenheimer surface. Remarkably, the configuration in Fig. 1(c) corresponds to minimum energy configuration [i.e., $E = -3.39$ eV relative to Fig. 1(a)], where H₂O is completely dissociated into one O atom, which is adsorbed to two fourfold Mo atoms and two H atoms which are adsorbed to two different twofolded S atoms in the same S plane. Transition state calculations find energy barriers of 99 and 218 meV to split H from OH in Fig. 1(b) and to change to the configuration in Fig. 1(f) and then to settle in Fig. 1(c).
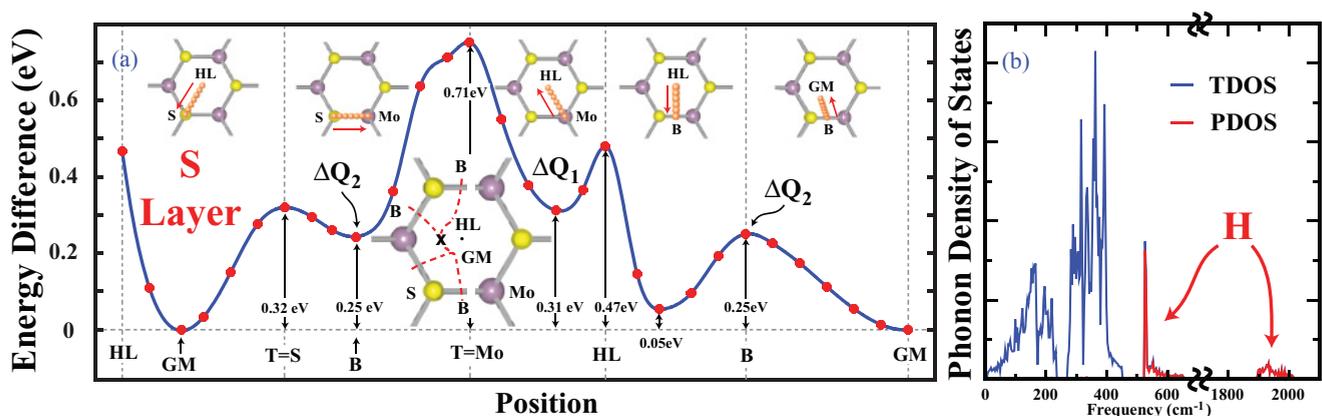

FIG. 2. (Color online) (a) Variation of the total energy of a single isolated H adatom migrating on the surface along the special directions of the 1H-MoS₂ honeycomb structure. Purple (large gray), yellow (light), and orange (small light gray) balls indicate Mo, S, and H atoms, respectively. Each red dot corresponds to the minimum total energy of H on the 1H-MoS₂ surface at a fixed x- and y-lateral position, but its height z together with all atomic positions of 1H-MoS₂ are optimized. B, T, HL, and GM indicate bridge, top (of S and Mo), hollow, and geometric minimum sites, respectively. The migration path of a single H is shown by dashed red lines on a hexagon. Relevant energy barriers are indicated by ΔQ_1 (occurs between HL-T = Mo indicated by "x") and ΔQ_2 (occurs at B sites). (b) Total density of states (TDOS) of phonon frequencies of single H adsorbed to 1H-MoS₂ together with the density of states projected to the modes of a H atom (PDOS) are used to estimate the characteristic jump frequency ν.

Two of the remaining configurations correspond to the water molecule, which is completely split as in Fig. 1(c); the third one is similar to Fig. 1(b). In these configurations the Mo-O-Mo bonds are ionic, where the effective charges on Mo and O are $+1.25e$ and $-0.90e$, respectively. As for the S-H bond, which is formed from the combination of the s orbital of H and the p_z and p_x orbitals of S with a transfer of $\sim 0.1e$ from H to S. A magnetic moment of $2\mu_B$ is attained due to unpaired electrons in these configurations. In addition to the states in Figs. 1(b)–1(f), H atoms can be bound also to the Mo layer with relatively low binding energy.

Whether a second H_2O molecule can be bound and subsequently split in the same MoS_2 vacancy, is also explored by a similar analysis. As a matter of fact, the second water molecule can be trapped in the vacancy and is bonded to the second dangling bond of fourfolded Mo atoms, which already hold the first one. Concomitantly, a H atom is released from H_2O and moved to another twofolded S atom leaving behind an OH bonded to Mo atom. However, this OH cannot be further split into O and H, since Mo atoms cannot donate sufficient electrons to the second O. Hence, H is needed to supply the required charge for the second O.

B. Diffusion of H atom on MoS_2 surface

Desorption of adsorbed H atoms from $1H\text{-}MoS_2$ may follow different reaction paths: (i) Hydrogen atoms can desorb by the breaking of the S-H bonds from twofolded S atoms surrounding the vacancy and eventually form H_2 to be released from $1H\text{-}MoS_2$. The S-H bond energies are 2.90–3.08 eV. In this process the S-H bonds can be broken using a photochemical process, which involves the calculation of an adsorption cross section for various incident angles of light photons, photoexcitation of electrons from bonding states to nonbonding states, and the expected desorption of H atoms. (ii) In a concerted process, while the S-H bonds around the vacancy are broken, H atoms are displaced and eventually can be adsorbed to the GM site (i.e., geometric minimum site near the center of the hexagon as shown in Fig. 2) with a relatively weaker binding energy of 0.78 eV. This process of bond breaking and rebonding requires an energy, which is relatively smaller than that in the first reaction path, namely, 2.12–2.30 eV. Therefore, the second path appears to be favorable. Once removed from the S-H bonds around vacancy and the adsorbed GM site on the surface of $1H\text{-}MoS_2$, H atoms diffuse readily on the surface of $1H\text{-}MoS_2$. An attractive interaction sets in between two H atoms when they are within a threshold distance. Eventually these two H atoms form a H_2 molecule by releasing 2.90 eV energy to the system. Owing to the weak repulsive interaction H_2 molecules are forced to escape from the surface.

In what follows we examine the latter reaction path in two complementary steps: (i) The energetics of adsorbed H atoms migrating on the surface are investigated by total energy calculations, where the x and y positions of a single H atom are fixed but its z coordinate and positions of all remaining Mo and S atoms in the supercell are optimized. The details and relevant results of these calculations are summarized in Fig. 2. Owing to the honeycomb symmetry, the energies are calculated at the B, T, HL, and GM sites (denoting respectively, bridge,

top (of S and Mo atoms), hollow, and geometric minimum sites) and over the connecting lines as shown by the insets of Fig. 2(a). The strongest binding of a H atom on the perfect S plane occurs at the GM site. There is a barrier along the path between HL and T = Mo of energy $\Delta Q_1 = 0.31$ eV. Hence, an open path, on which a H atom can migrate for a long distance has to overcome ΔQ_1. Note that a slightly lower barrier of $\Delta Q_2 = 0.25$ eV supports only a closed path, which can circulate only among adjacent hexagons. We note that apart from the migration of H atoms on the outer S planes the migration of a H atom from the Mo layer toward the outer S plane the minimum energy barrier is relatively larger and is 0.67 eV. The migration of a H atom confined to the Mo plane encounters an even higher barrier of 1.47 eV.

We now focus on the most likely process of diffusion on the outer S plane and estimate the characteristic jump frequency v
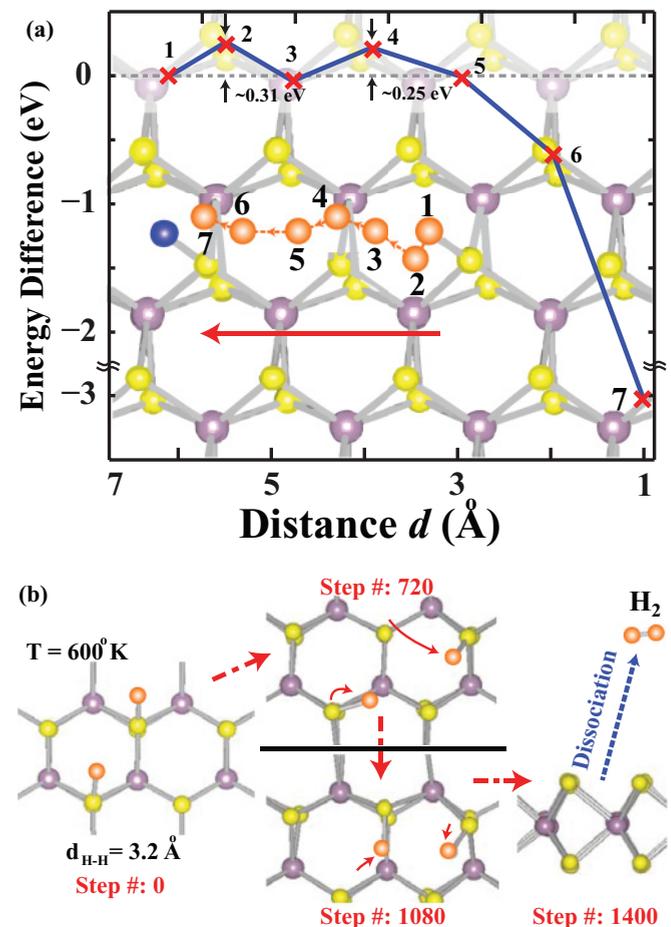
FIG. 3. (Color online) (a) The interaction energy between two hydrogen adatoms on $1H\text{-}MoS_2$; one is initially adsorbed at the GM site [shown by a blue (dark) ball] on the surface, the other [shown by an orange (light gray) ball] moves on the path of minimum energy barrier. Within the adatom-adatom distance of 1.97 Å H adatoms begin to interact. At the end both adatoms on $1H\text{-}MoS_2$ form a H_2 molecule and release from the surface. Purple (large gray) and yellow (light) balls are Mo and S atoms, respectively. (b) Relevant atomic structures corresponding to some intermediate steps of *ab initio* molecular dynamics calculations at $T = 600$ K. Initial distance between hydrogen atoms is taken as $d_{H\text{-}H} = 3.2$ Å longer than the threshold distance.

from phonon calculations. Using the density of phonon states, which are projected to the modes of H atoms in Fig. 2(b) we estimate $\nu = \sim 600$ cm^{-1}. Then, the diffusion constant $D = \nu a^2 \exp(-\Delta Q / k_B T)$ on the S plane is obtained to be 1.21×10^{-7} cm^2/s at room temperature (4.55×10^{-5} cm^2/s at 600 K). The calculated values indicate a high diffusion rate even at room temperature. Since the H atom, being the lightest atom, can be considered as a quantum particle, we explored the situation of how the diffusion of H atoms is enhanced through their tunneling the barrier. We found that the tunneling is relevant for only 10 meV barriers.

Having shown that H atoms attached on S atoms subsequent to the dissociation of H$_2$O diffuse readily on the outer S plane, the crucial question is how these H atoms can dissociate from 1H-MoS$_2$. Despite a 0.31 eV energy barrier across the diffusion path of individual H atoms, this barrier is weakened and eventually changes to an attractive interaction between two H atoms, when their separation becomes smaller than a threshold value. The calculation of interaction between two diffusing H atoms on the minimum energy path is outlined in Fig. 3(a). Two H atoms, while one of them with its (x, y) coordinates is forced to follow the minimum energy path in steps but optimizing its z coordinate, the other one and all the rest of the Mo and S atoms are fully relaxed. Once the separation between two H atoms becomes smaller than the threshold distance, the attractive interaction facilitates the formation of H$_2$. Eventually, at a separation smaller than 2 Å, a H$_2$ is formed spontaneously by releasing 2.90 eV at 0 K. Owing to the weak repulsive interaction a H$_2$ molecule escapes from the surface. In Fig. 3(b) the diffusion and formation of H$_2$ having a H-H distance larger than the threshold distance is simulated by *ab initio* MD calculations at $T = 600$ K.

IV. DISCUSSIONS AND CONCLUSIONS

In conclusion, we demonstrated that a free water molecule is attracted by a MoS$_2$ vacancy of 1H-MoS$_2$ and is trapped in the hole. Concomitantly, H$_2$O is dissociated into constituent O and H atoms. While an O atom remains to be bonded to the dangling bonds of two Mo atoms around vacancy, H atoms are preferably attached to twofolded S atoms surrounding the vacancy. Once H atoms bound to S atoms around the vacancy are transferred to GM sites by any process, these H atoms diffuse readily and form a H$_2$ molecule spontaneously. That the ionization energy of Mo is smaller than that of H, so that it donates electrons to O to free H atoms is crucial for the spontaneous dissociation of the water molecule. In this paper, we are concerned only with catalytic reactions resulting in the dissociation of H$_2$O at a MoS$_2$ vacancy and diffusion of H atoms freed from vacancy on the surface of 1H-MoS$_2$. The diffusing H atoms readily form H$_2$ molecules and eventually are desorbed from the surface. The phenomena involving bond breaking through photochemical processes leading directly to H$_2$ evaluation from the vacancy or various concerted processes requiring energy relatively smaller than the former case and eventually leading to the transfer of a H atom to the GM site on the surface are complex and need to be analyzed extensively. These studies will be the subject matter of our forthcoming papers.

While advances in nanotechnology can provide us 1H-MoS$_2$ with high vacancy concentration, the removal of O bound to Mo through charging or other means can allow us recyclable use of the same system. Because of exceptional properties similar to one revealed in this paper, single-layer MoS$_2$ honeycomb structure has been considered as a contender of graphene. A recent study showed that several transition-metal dichalcogenides form similar stable single-layer honeycomb structures[27] and are potential candidates for similar catalytic reactions. The kinetics in the process above can be monitored by applied potential difference. We believe that the catalytic reaction predicted in this work heralds a sustainable and clean energy resource and will initiate several experimental studies.

---

[*]ciraci@fen.bilkent.edu.tr

[1]R. Coontz and B. Hanson, Science **309**, 957 (2004).

[2]S. Dag, Y. Ozturk, S. Ciraci, and T. Yildirim, Phys. Rev. B **72**, 155404 (2005).

[3]T. Yildirim and S. Ciraci, Phys. Rev. Lett. **94**, 175501 (2005).

[4]E. Durgun, S. Ciraci, W. Zhou, and T. Yildirim, Phys. Rev. Lett. **97**, 226102 (2006).

[5]C. Ataca, E. Akturk, S. Ciraci, and H. Ustunel, Appl. Phys. Lett. **93**, 043123 (2008); C. Ataca, E. Aktürk, and S. Ciraci, Phys. Rev. B **79**, 041406 (2009).

[6]*Metal Dihydrogen and Bond Complexes—Structure, Theory and Reactivity*, edited by K. J. Kubas (Kluwer Academic-Plenum, New York, 2001).

[7]B. Hinnemann, P. G. Moses, J. Bonde, K. P. Jorgensen, J. H. Nielsen, S. Horch, I. Chorkendorff, and J. K. Norskov, J. Am. Chem. Soc. **127**, 5308 (2005).

[8]X. Zong, G. Wu, H. Yan, G. Ma, J. Shi, F. Wen, L. Wang, and C. Li, J. Phys. Chem. C **114**, 1963 (2010).

[9]J. Bonde, P. G. Moses, T. F. Jaramillo, J. K. Norskov, and I. Chorkendorff, Faraday Discuss. **140**, 219 (2009).

[10]D. Merki, S. Fierro, H. Vrubel, and X. Hu, Chem. Science **2**, 1262 (2011).

[11]P. G. Moses, B. Hinnemann, H. Topsoe, and J. K. Norskov, J. Catal. **248**, 188 (2007).

[12]J. Greeley, T. F. Jaramillo, J. Bonde, I. Chorkendorff, and J. K. Norskov, Nature Mater. **5**, 909 (2006).

[13]J. K. Norskov, T. Bligaard, A. Logadottir, J. R. Kitchin, J. G. Chen, S. Pandelov, and U. Stimming, J. Electrochem. Soc. **152**, J23 (2005).

[14]J. K. Norskov, T. Bligaard, J. Rossmeisl, and C. H. Christensen, Nat. Chem. **1**, 37 (2009).

[15]Y. Li, H. Wang, L. Xie, Y. Liang, G. Hong, and H. Dai, J. Am. Chem. Soc. **133**, 7296 (2011).

[16] Y. Sasaki, H. Nemoto, K. Saito, and A. Kudo, J. Phys. Chem. C **113**, 17536 (2009).

[17] A. Kudo, H. Kato, and S. Nakagawa, J. Phys. Chem. B **104**, 571 (2000).

[18] A. Iwase, Y. H. Ng, Y. Ishiguro, A. Kudo, and R. Amal, J. Am. Chem. Soc. **133**, 11054 (2011).

[19] K. Maeda, R. Abe, and K. Domen, J. Phys. Chem. C **115**, 3057 (2011).

[20] M. V. Bollinger, K. W. Jacobsen, and J. K. Norskov, Phys. Rev. B **67**, 085410 (2003).

[21] T. F. Jaramillo, K. P. Jorgensen, J. Bonde, J. H. Nielsen, S. Horch, and I. Chorkendorff, Science **317**, 100 (2007).

[22] J. V. Lauritsen, J. Kibsgaard, S. Helveg, H. Topsoe, B. S. Clausen, E. Laegsgaard, and F. Besenbacher, Nat. Nanotechnol. **2**, 53 (2007).

[23] K. F. Mak, C. Lee, J. Hone, J. Shan, and T. F. Heinz, Phys. Rev. Lett. **105**, 136805 (2010).

[24] C. Ataca, H. Şahin, E. Aktürk, and S. Ciraci, J. Phys. Chem. C **115**, 3934 (2011). In this paper an extensive list of references for experimental and theoretical works related with MoS_2 is presented.

[25] C. Ataca and S. Ciraci, J. Phys. Chem. C **115**, 13303 (2011).

[26] C. Ataca, M. Topsakal, E. Aktürk, and S. Ciraci, J. Phys. Chem. C **115**, 16354 (2011).

[27] C. Ataca, H. Şahin, and S. Ciraci, J. Phys. Chem. C **116**, 8983 (2012). In this paper all single-layer transition-metal dichalcogenide structures, 1H-MX_2 and 1T-MX_2 (M = transition-metal atom and X = O, S, Se, and Te) which are found to be stable and their relevant properties are reported.

[28] B. Radisavljevic, A. Radenovic, J. Brivio, V. Giacometti, and A. Kis, Nat. Nanotechnol. **6**, 147 (2011).

[29] T. Li and G. Galli, J. Phys. Chem. C **111**, 16192 (2007).

[30] S. Cahangirov, C. Ataca, M. Topsakal, H. Sahin, and S. Ciraci, Phys. Rev. Lett. **108**, 126103 (2012).

[31] J. Bai, X. Zhong, S. Jiang, Y. Huang, and X. Duan, Nat. Nanotechnol. **5**, 190 (2010).

[32] J. Lahiri, Y. Lin, P. Bozkurt, I. I. Oleynik, and M. Batzill, Nat. Nanotechnol. **5**, 326 (2010).

[33] R. Balog, B. Jorgensen, L. Nilsson, M. Andersen, E. Rienks, M. Bianchi, M. Fanetti, E. Laegsgaard, A. Baraldi, S. Lizzit, Z. Sljivancanin, F. Besenbacher, Bjork Hammer, T. G. Pedersen, P. Hofmann, and L. Hornekaer, Nature Mater. **9**, 315 (2010).

[34] P. E. Blochl, Phys. Rev. B **50**, 17953 (1994).

[35] J. P. Perdew, K. Burke, and M. Ernzerhof, Phys. Rev. Lett. **77**, 3865 (1996).

[36] S. Grimme, J. Comput. Chem. **27**, 1787 (2006).

[37] G. Henkelman, A. Arnaldsson, and H. Jonsson, Comput. Mater. Sci. **36**, 354 (2006).

[38] G. Kresse and J. Hafner, Phys. Rev. B **47**, 558 (1993); G. Kresse and J. Furthmuller, Phys. Rev. B **54**, 11169 (1996).

[39] D. Alfe, Comput. Phys. Commun. **180**, 2622 (2009).